Second International Conference
"Tropical Climatology, Meteorology and Hydrology"
Proceedings edited by
G. Demarée, M. De Dapper, J. Alexandre
pp. 27-40 (2004)

Preliminary Results of a Reduced-gravity Model of the Wind-induced Oscillations of the Thermocline in Lake Tanganyika

by

Jaya NAITHANI*, Eric DELEERSNIJDER*,
Pierre-Denis PLISNIER**,*** & Sébastien LEGRAND*,****

KEYWORDS. — Lake Tanganyika ; Thermocline ; Internal Seiche ; Reduced-gravity Model.

SUMMARY. — A two-dimensional, reduced-gravity model is established to study the wind-induced oscillations of the thermocline of Lake Tanganyika. An analytical solution is obtained for a simplified, one-dimensional, linearized set of equations, which suggests that the first mode of oscillation — exhibiting one node only — should be dominant. The sensitivity to the wind stress, the stratification and the unperturbed thermocline depth of the amplitude and period of the linear solution is analysed. Numerical solutions of the complete, non-linear, two-dimensional reduced-gravity model are compared cursorily with field data and are seen to exhibit properties that are rather similar to those of the idealized, one-dimensional model.

1. Introduction

Lake Tanganyika is one of the deepest freshwater lakes in the world with a maximum depth of about 1,470 m. The lake is situated from

* Institut d'Astronomie et de Géophysique G. Lemaître, Université Catholique de Louvain, 2 Chemin du Cyclotron, B-1348 Louvain-la-Neuve (Belgium).
** Geology and Mineralogy Department, Royal Museum for Central Africa, 13 Leuvensesteenweg, B-3080, Tervuren (Belgium).
*** Laboratoire d'Ecologie des Eaux Douces, Facultés Universitaires Notre-Dame de la Paix, 61 rue de Bruxelles, B-5000 Namur (Belgium).
**** Centre for Systems Engineering and Applied Mechanics, Université Catholique de Louvain, 4 Avenue G. Lemaître, B-1348 Louvain-la-Neuve (Belgium).

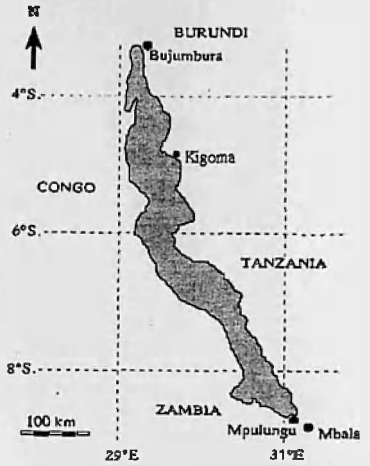

Fig. 1. — Map of Lake Tanganyika

3°20' S to 8°45' S, and 29°05' E to 31°15' E (fig. 1). On average, its length and width are of the order of 650 km and 50 km, respectively. The lake is a significant source of food for the countries sharing it, *i.e.* DR Congo, Burundi, Tanzania and Zambia. The region undergoes two main seasons, the dry season and the wet season. The dry season, approximately from May to September, is characterized by strong southeasterly winds, the trade winds, whereas during the wet season the winds are generally northeasterly and weaker (COULTER & SPIGEL 1991), though some short, strong wind events can occur during this season. For the dry seasons of ENSO years, preliminary data suggest that the air temperature is higher and the wind weaker. This seems to cause variability in catches of several species of pelagic fishes, affecting the economy and the food stock of the neighbouring populations (PLISNIER 1997, PLISNIER *et al.* 2000). Furthermore, over recent years, the lake hydrodynamics has been seen to exhibit variability related to climate change (PLISNIER 1997, 2000).

Understanding the lake hydrodynamics and its variability is important for the management of its resources, as well as understanding limnological conditions in the framework of paleoclimatic studies such as the ongoing CLIMLAKE project (DESCY *et al.* 2002). In this respect, numerical modelling is an invaluable tool. Our objective is to build a three-dimensional model of the lake hydrodynamics and ecology. The first stage of this undertaking is concerned with the study of one of the most striking features of the lake hydrodynamics, *i.e.* the tilting of thermocline occurring during the dry season and the associated large-amplitude internal seiches (COULTER & SPIGEL 1991, CHITAMWEBWA 1999, PLISNIER *et al.* 1999, PLISNIER & COENEN 2001). These phenomena, which are believed to be induced by the wind forcing, are studied herein by means of a reduced-gravity model.

In the next section, the equations and the surface forcing of the reduced-gravity model are established. Then, this model is simplified to a one-dimensional, linear model, of which an analytical solution is derived and analysed. Finally, numerical results of the complete reduced-gravity model are obtained, and compared cursorily with field data and one-dimensional, analytical solutions.

2. The Reduced-gravity Model

The thermocline is present all year round over a large fraction of the lake. This is the main reason why a two-layer model is believed to be a relevant tool for representing the motions of the thermocline in an idealized manner. In such a model, the prognostic variables related to each layer are assumed to be vertically homogeneous. If the subscripts "1" and "2" are associated with the top and the bottom layer, respectively, h_i, u_i and v_i ($i = 1,2$) denote, for the i-th layer, the unperturbed depth, the component of the horizontal velocity along the x-axis and the component of the horizontal velocity along the y-axis, x and y being Cartesian horizontal coordinates as illustrated in figure 2. Let η and ξ represent the upward displacement of the lake surface and the downward displacement of the thermocline, respectively, which is assumed to be impermeable (fig. 3). If the pycnocline and bottom stresses are neglected, the continuity and horizontal momentum equations read :

$$\frac{\partial H_1}{\partial t} + \nabla \bullet (H_1 \mathbf{u}_1) = 0, \tag{1}$$

$$\frac{\partial (H_1 \mathbf{u}_1)}{\partial t} + \nabla \bullet (H_1 \mathbf{u}_1 \mathbf{u}_1) + f \mathbf{e}_z \times (H_1 \mathbf{u}_1) = -gH_1 \nabla \eta + \mathbf{D}_1 + \frac{\mathbf{t}}{\rho_1}, \tag{2}$$

$$\frac{\partial H_2}{\partial t} + \nabla \bullet (H_2 \mathbf{u}_2) = 0, \tag{3}$$

$$\frac{\partial (H_2 \mathbf{u}_2)}{\partial t} + \nabla \bullet (H_2 \mathbf{u}_2 \mathbf{u}_2) + f \mathbf{e}_z \times (H_2 \mathbf{u}_2) = -gH_2 \nabla (\eta - \varepsilon \xi) + \mathbf{D}_2, \tag{4}$$

where t is time ; $\mathbf{u}_i = u_i\mathbf{e}_x + v_i\mathbf{e}_y$ is the velocity vector in the i-th layer ; $\mathbf{e}_x$ and $\mathbf{e}_y$ are the horizontal unit vectors associated with the x and y coordinate axes, while $\mathbf{e}_z = \mathbf{e}_x \times \mathbf{e}_y$ is the vertical unit vector, pointing upward ; f is the Coriolis factor — which is relatively small and negative in the domain of interest — and g is the gravitational acceleration (≈ 9.8 m s^{-2}).

In the governing equations above, the vector is the wind stress, which is evaluated by means of the Smith & Banke (1975) parameterization,

$$\mathbf{t} = \rho_a\,(0.63 \times 10^{-3} + 0.066 \times 10^{-3}|\mathbf{v}_a|)\,|\mathbf{v}_a|\,\mathbf{v}_a\,, \qquad (5)$$

where ρ_a (≈ 1 kg m^{-3}) is the air density and $\mathbf{v}_a$ is the wind velocity, expressed in m s^{-1}. The actual height of each water layer is evaluated as $H_1 = h_1 + \eta + \xi$ and $H_2 = h_2 - \xi$. The dissipative terms are expressed as

$$\mathbf{D}_i = \nabla \bullet (A_x H_i \nabla u_i) + \nabla \bullet (A_y H_i \nabla v_i) \quad (i = 1,2), \qquad (6)$$

where A_x and A_y are the horizontal eddy viscosities, which are taken to be different in the x- and y-directions because the "width" of the lake is much smaller than its "length". If the constant ρ_i ($i = 1,2$) represents the water density in the i-th layer, the relative density difference ε is defined to be

$$\varepsilon = \frac{\rho_2 - \rho_1}{\rho_2}\,. \qquad (7)$$

The density is computed from the UNESCO (1981) equation of state of the water, in which the salinity is set to zero while the pressure is assumed to be equal to one atmosphere — as density variations are mainly due to temperature variations in Lake Tanganyika. Given the range of the available *in situ* temperature profiles, ε is likely to be smaller than 10^{-3}.

The displacement of the lake surface is assumed to be much smaller than that of the pycnocline. Therefore, by virtue of continuity equations (1) and (3), the layer heights and transports satisfy $\partial H_1/\partial t \approx -\partial H_2/\partial t \approx -\nabla \bullet (H_1\mathbf{u}_1) \approx \nabla \bullet (H_2\mathbf{u}_2)$. Thus, the order of magnitude of the top layer transport, $H_1\mathbf{u}_1$, is equal to that of the bottom layer, $H_2\mathbf{u}_2$, implying that the order of magnitude of the left-hand side of momentum equation (2) is equivalent to that of the left-hand side of (4). As the thickness of the hypolimnion ranges from about 100 m to over 1,000 m while the depth of the epilimnion rarely exceeds 50 to 100 m, the ratio H_1/H_2 is generally much smaller than unity. Therefore, the contributions to the pressure force prevailing in the hypolimnion are likely to be the only dominant terms in (4), *i.e.* $-gH_2\nabla(\eta - \varepsilon\xi) \approx 0$. By virtue of continuity equations (1) and (3), the lake-averaged values of η and ξ must be constants, which are

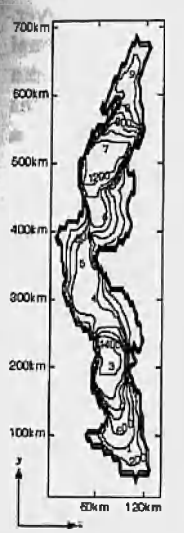

Fig. 2. — Bathymetry (in metres) of Lake Tanganyika.

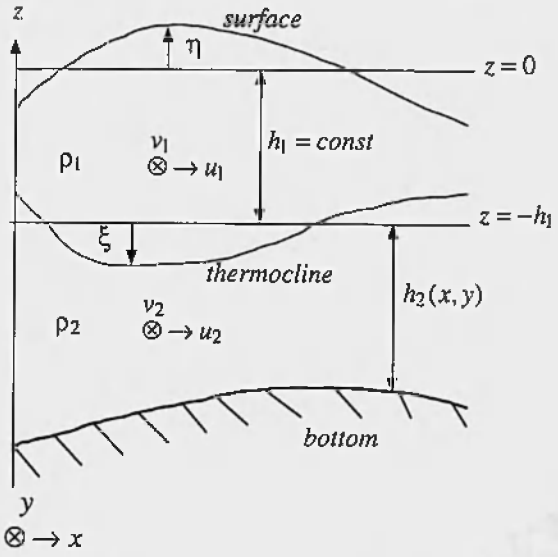

Fig. 3. — The main parameters and variables of a two-layer model of the lake, which upon assuming that $h_1 \ll h_2$ gives rise to a reduced-gravity model.

assumed to be zero in all applications considered below. As a result, the displacement of the lake surface and that of the thermocline satisfy approximately the following relation

$$\eta = \varepsilon\xi\,. \qquad (8)$$

Substituting (8) into the pressure force in the right-hand side of (2), neglecting η relative to ξ, dropping the subscripts "1", it is readily seen that the equations governing the dynamics of the epilimnion can be approximated by

$$\frac{\partial H}{\partial t} + \nabla \bullet (H\mathbf{u}) = 0, \qquad (9)$$

$$\frac{\partial (H\mathbf{u})}{\partial t} + \nabla \bullet (H\mathbf{u}\mathbf{u}) + f\mathbf{e}_z \times \mathbf{u} = -\varepsilon g H \nabla\xi + \mathbf{D} + \frac{\mathbf{t}}{\rho}\,, \qquad (10)$$

with $H = h + \xi$. The latter equations are similar to those of a one-layer, depth-integrated model, except for the reduction of the gravitational acceleration by the small dimensionless factor ε. Hence, they make up a model usually referred to as "reduced-gravity model". Models of this type have demonstrated their ability to represent the displacement of a pycnocline in many applications.

3. The Linearized, One-dimensional Model

According to NAITHANI *et al.* (2002), a suitable idealized wind forcing is as follows : during the wet season the wind stress is zero, and during the dry season the wind is assumed to blow at a constant velocity from the southern end of the lake toward the northern one. Let T_d and T_w denote the duration of the dry season and that of the wet season, respectively, so that one year is $T = T_d + T_w$. Then, if time is prescribed to be zero at the beginning of a dry season, the wind stress can be written as $\mathbf{t} = t_y(t)\mathbf{e}_y$, with

$$t_y(t) = \sum_{j=0}^{\infty} [\chi(t - jT) - \chi(t - jT - T_d)]\rho\tau , \qquad (11)$$

where ρτ is a positive constant representing the dry season wind stress, which is to be estimated by means of parameterization (5), knowing the order of magnitude of the wind speed ; χ is the Heaviside step function, *i.e.* a function which is equal to 1, 1/2, or 0, according to whether its argument is > 0, = 0, < 0. The surface forcing (11) (fig. 4) is used to obtain all of the results presented herein, be they of an analytical or a numerical nature.

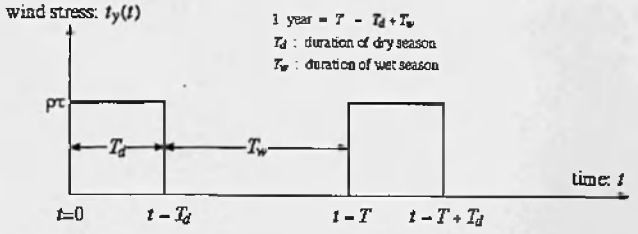

Fig. 4. — Schematic representation of the annual cycle of the wind stress (11).

Assuming that the thermocline displacement remains small compared with the thickness of the epilimnion, neglecting the Coriolis force and the advective part of the acceleration, integrating governing equations (9)-(10) over the width of the lake and parameterizing the dissipative terms as Newtonian friction — for physical reasons and for the sake of simplicity, as well —, the following linearized, one-dimensional model focused on along-lake variations is obtained :

$$\frac{\partial \xi}{\partial t} + h\frac{\partial v}{\partial y} = 0, \qquad (12)$$

$$\frac{\partial v}{\partial t} = -\varepsilon g\frac{\partial \xi}{\partial y} - \gamma v + \frac{t_y}{\rho h}, \qquad (13)$$

where γ is the relevant Newtonian friction coefficient. At the initial instant the thermocline displacement and the velocity are assumed to be zero. The impermeability of the lake ends requires that the velocity be prescribed to be zero at any time at both ends of the lake, *i.e.* $v(t, y = 0) = 0 = v(t, y) = L$, where $L = 650$ km is the length of the lake.

The steady-state response of the thermocline to the dry season wind stress ρτ is a linear function of the distance y to the southernmost end of the lake, with the thermocline being shallower in the south and deeper in the north, *i.e.*

$$\xi^s(y) = \left(\frac{2y}{L} - 1\right)\frac{L\tau}{2\varepsilon g h}, \qquad (14)$$

The associated along-lake velocity is obviously zero. This solution is incompatible with the initial conditions and, hence, cannot set in abruptly. For this reason, a transient regime develops, in which oscillations of the thermocline are superimposed on the steady-state solution. The response to a Heaviside-type wind forcing starting at $t = 0$ reads

$$\xi^H(t, y) = \xi^s(y) + \sum_{n=1}^{\infty} E_n e^{-\mu t}\left[\cos(\omega_n t) + \frac{\mu}{\omega_n}\sin(\omega_n t)\right]\cos(k_n y), \qquad (15)$$

$$v^H(t, y) = \sum_{n=1}^{\infty} V_n e^{-\mu t}\sin(\omega_n t)\sin(k_n y), \qquad (16)$$

with

$$E_n = \frac{4\tau}{\varepsilon g h L k_n^2} \quad \text{and} \quad V_n = \frac{4\tau}{hL\omega_n k_n}, \qquad (17)$$

where the damping coefficient, the angular frequency and the wave number of the n-th mode are $\mu = \gamma / 2$, $\omega_n = (\varepsilon g k h_n^2 - \mu^2)^{1/2}$ and $k_n = (2n - 1)\pi / L$, respectively. As the model is linear and the surface wind stress is a sum of Heaviside functions, the solutions of (11)-(13) may be expressed as a sum of appropriately-delayed responses to a single Heaviside-type forcing, *i.e.*

$$\xi(t, y) = \sum_{j=0}^{\infty} [\xi^H(t - jT, y)\chi(t - jT) - \xi^H(t - jT - T_d, y)\chi(t - jT - T_d)], \quad (18)$$

$$v(t, y) = \sum_{j=0}^{\infty} [v^H(t - jT, y)\chi(t - jT) - v^H(t - jT - T_d, y)\chi(t - jT - T_d)]. \quad (19)$$

The oscillations of the thermocline may be seen as standing waves, of which the n-th mode exhibits $2n - 1$ nodes. As $E_n / E_1 = (2n - 1)^{-2}$, the amplitudes E_n of the oscillation modes decrease quickly as n increases, so that only the first mode contributes significantly to the oscillations, as is illustrated in figure 5. In other words, the present simplified model suggests that the thermocline oscillations are likely to exhibit only one node, in the centre of the lake, and two maxima, at the ends of the lake.

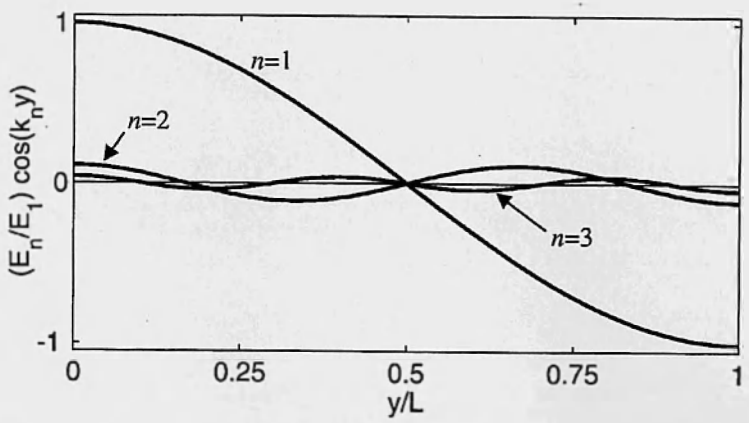

Fig. 5. — The first three modes (n = 1,2,3) of the thermocline oscillations, as defined in expressions (15) and (17).

Furthermore, according to the idealized solution above, the amplitude and period of thermocline oscillations should depend on the wind stress, the density difference — or stratification — and the unperturbed depth of the thermocline as indicated in table 1, and exhibit values of the order of those displayed in figure 6. The latter suggests that the period of the oscillations is much less sensitive than the amplitude of the thermocline motions to the variations of the model parameters and forcing.

Table 1

Qualitative illustration of the sensitivity of the amplitude and period of thermocline oscillations to model parameters or forcing, in accordance with the linearized, one-dimensional model solution

	Amplitude	Period
Wind velocity : $v_a \uparrow$	↑	—
Stratification : $\varepsilon \uparrow$	↓	↓
Unperturbed depth of the thermocline : $h \uparrow$	↓	↓

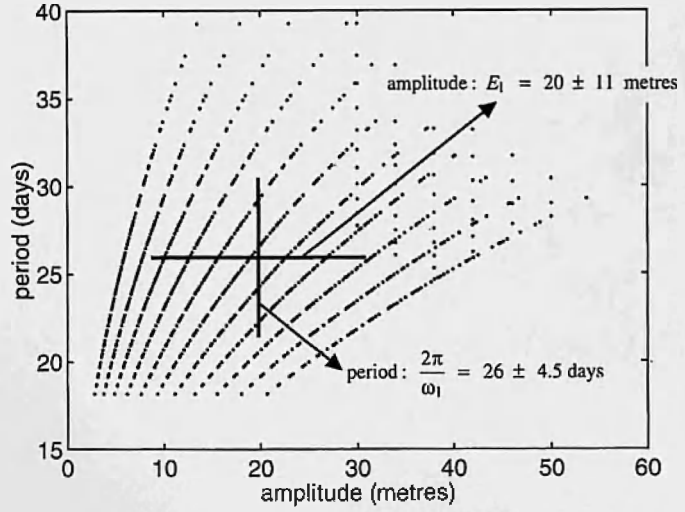

Fig. 6. — Values of the amplitude E_1 and period $2\pi / \omega_1$ of the first — and only significant — mode of thermocline oscillations obtained by varying the wind velocity v_a, the relative density difference ε and the unperturbed depth of the thermocline h in the intervals $3 \leq v_a \leq 7$ (m s^{-1}), $0.5 \times 10^{-3} \leq \varepsilon \leq 10^{-3}$ and $30 \leq h \leq 70$ (m), which are believed to represent the range of the admissible values of these parameters. The damping coefficient μ is set to 2 year^{-1}, a value which has a minor impact on the amplitude and period of the oscillations — but seems to be appropriate in view of the numerical results discussed below. The mean and standard deviation of amplitude E_1 and period $2\pi / \omega_1$ are indicated.

4. Numerical Results from the Complete Reduced-gravity Model

The equations (9)-(10) of the complete reduced-gravity model are discretized on an Arakawa C-grid, and solved by means of a finite-volume scheme including a forward-backward time stepping similar to that described in BECKERS & DELEERSNIJDER (1993). The "width" of the lake being much smaller than its "length", the grid size in the x-direction is set to be smaller than that associated with the y-direction, *i.e.* $\Delta x = 3$ km and $\Delta y = 10$ km. To ensure numerical stability, the time increment Δt must be such as that (BECKERS & DELEERSNIJDER 1993).

$$\Delta t \leq \max \left\{ \frac{1}{|f|}, \frac{\Delta x \Delta y}{[2gh(\Delta x^2 + \Delta y^2)]^{1/2}} \right\}. \qquad (20)$$

It is readily seen that setting $\Delta t = 5$ minutes is appropriate for most relevant values of the model parameters. For numerical reasons, the horizontal viscosities are given values satisfying $A_y / A_x = \Delta y^2 / \Delta x^2$. A series of numerical experiments suggests that the suitable order of magnitude of A_y is 3 m^2 s^{-1}.

In certain model runs, the upward displacement of the thermocline can be equivalent to the unperturbed depth of the thermocline. To prevent the thermocline from outcropping, an elementary wetting-drying algorithm

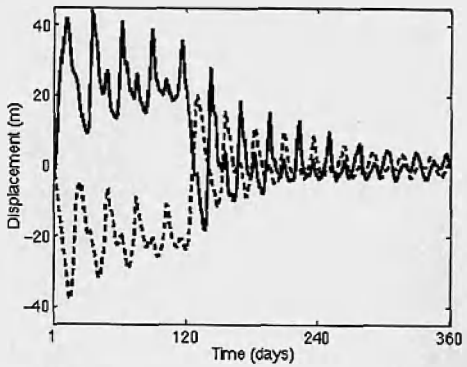

Fig. 7. — Evolution during the second year of simulation of the downward displacement of the thermocline at the northern (solid curve) and southern (dashed curve) ends of the lake, as evaluated by means of the complete, reduced-gravity model. The unperturbed depth of the thermocline, the dry season duration, the wind speed, and the relative density difference are $h = 50$ m, $T_d = 4$ months, $v_a = 5$ m s^{-1}, and $\varepsilon = 6.3 \times 10^{-4}$, respectively.

(BALZANO 1998) is implemented, consisting in setting to zero the water fluxes crossing the boundaries of every grid box in which the actual water column depth would become — after one-time step — smaller than a critical value, which is taken to be 5 m herein.

A series of numerical experiments is conducted, with different values of the model parameters, the results of which are in agreement with table 1. A detailed discussion of this work may be found in NAITHANI *et al.* (2002), along with an in-depth comparison with the available field data, which includes the identification of the main timescales of the thermocline displacement by means of wavelet analysis. Typical numerical results are displayed in figure 7. The latter is qualitatively and — to a large extent — quantitatively similar to the analytical solution of the linear model presented in figure 8, indicating the relevance of the analytical solution (18). The tilting of the thermocline induced by the dry season wind stress — from day 1 to day 120 in figures 7 and 8 —, and the oscillations of the thermocline may be found in all available field data, as may be seen in, for instance, COULTER & SPIGEL (1991), NAITHANI *et al.* (2002) and figure 9.

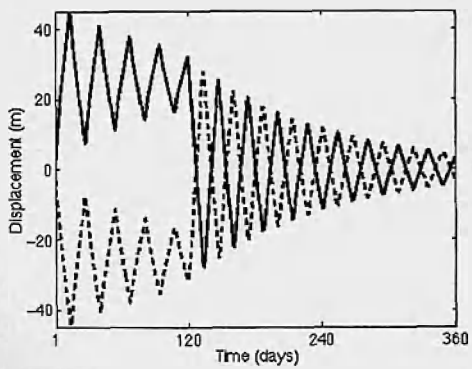

Fig. 8. — Evolution during the second year of calculation of the downward displacement of the thermocline at the northern (solid curve) and southern (dashed curve) ends of the lake, as obtained from the analytical solution (18) of the simplified, linearized model. The model parameters listed in the caption to figure 7 are equal to those selected to obtain the present results. In addition, the friction parameter γ is set to 4 year^{-1}.

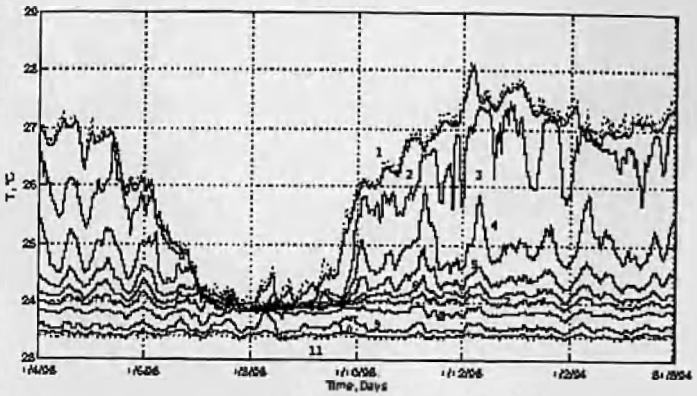

Fig. 9. — Time series of the temperature measured in 1993-1994 at various depths in the vicinity of Mpulungu. The numbers 1 to 11 correspond to the depths 1, 5, 30, 50, 70, 90, 110, 150, 200, 250 and 300 m. These data are from FAO/FINNIDA.

5. Conclusions

The analytical solution and the numerical results of the complete, reduced-gravity model are capable of reproducing the dry-season tilting of the thermocline — with the latter being deeper in the northern part of the lake — and the oscillations of the thermocline, which are present all year round, are largely dominated by the mode exhibiting only one node in the neighbourhood of the middle of the lake, and have a main period and an amplitude of the order of 3 to 4 weeks and a few tens of metres, respectively. The mixing due to wind-induced turbulence is not represented by the models dealt with herein, and will be addressed in the near future by a three-dimensional, hydrodynamic model including a turbulence closure scheme. The latter will be coupled with an ecological model.

ACKNOWLEDGEMENTS

The present work is carried out in the scope of the project "Climate Variability as Recorded in Lake Tanganyika" (CLIMLAKE), which is funded by the Belgian Federal Office for Scientific, Technical and Cultural Affairs under contract EV/10/2D. Eric Deleersnijder is a Research Associate with the Belgian National Fund for Scientific Research (FNRS). Figure 9 data are from the FAO/FINNIDA project LTR. The authors are indebted to A. Dierickx, P. Tréfois and D. Delvaux of the Royal Museum for Central Africa for producing a digital bathymetry of Lake Tanganyika.

REFERENCES

Balzano, A. 1998. Evaluation of methods for numerical simulation of wetting and drying in shallow water flow models. — *Coastal Engineering*, **34** : 83-107.

Beckers, J. M. & Deleersnijder, E. 1993. Stability of a FBTCS scheme applied to the propagation of shallow-water inertia gravity waves on various space grids. — *Journal of Computational Physics*, **108** (1) : 95-104.

Chitamwebwa, D. B. R. 1999. Meromixis, stratification and internal waves in Kigoma waters of Lake Tanganyika. — *Hydrobiologia*, **407** : 59-64.

Coulter, G. W. &. Spigel, R. H. 1991. Hydrodynamics. — *In* : Coulter, G. W. (Ed.), Lake Tanganyika and its Life, Oxford University Press, pp. 49-75.

Descy, J.-P., Plisnier, P.-D., Andre, L., Alleman, L., Chitamwebwa, D., Cocquyt, C., Deleersnijder, E., Kimirei, I., Naithani, J., Phiri, H., Sinyenza, D. & Vyverman, W. 2002. Climate variability as recorded in Lake Tanganyika (CLIMLAKE). — *Bulletin of the International Decade for the East African Lakes*, pp. 7-8.

Naithani, J., Deleersnijder, E. & Plisnier, P.-D. 2002. Analysis of wind-induced thermocline oscillations of Lake Tanganyika — *Environmental Fluid Mechanics*, **3** : 23-39.

Plisnier, P.-D. 1997. Climate, Limnology and Fisheries Changes of Lake Tanganyika. — FAO/FINNIDA Research for the Management of the Fisheries on Lake Tanganyika. GCP/RAF/271/FIN-TD/73(En), 50 pp.

Plisnier, P.-D. 2000. Recent climate and limnology changes in Lake Tanganyika. — *Verh. Internat. Verein. Limnol.*, **27** : 2670-2673.

Plisnier, P.-D., Chitamwebwa, D., Mwape, L., Tshibangu, K., Langenberg, V. & Coenen, E. 1999. Limnological annual cycle inferred from physical-chemical fluctuations at three stations of Lake Tanganyika. — *Hydrobiologia*, **407** : 45-58.

Plisnier, P.-D. & Coenen, E. 2001. Pulsed and dampened annual limnological fluctuations in Lake Tanganyika. — *In* : Munawar, M. H. (Ed.), The Great Lakes of the World (GLOW) : Foodweb, Health and Integrity, *Backhuys*, pp. 83-96.

Plisnier, P.-D., Serneels, S. & Lambin, E. F. 2000. Impact of ENSO on East African ecosystems : a multivariate analysis based on climate and remote sensing data. — *Global Ecology and Biogeography*, **9** (6) : 481-497.

Smith, S. D. & Banke, E. G. 1975. Variation of the sea surface drag coefficient with wind speed. — *Quarterly Journal of the Royal Meteorological Society*, **101** : 665-673.

UNESCO 1981. Tenth Report of the Joint Panel on Oceanographic Tables and Standards. — UNESCO Technical Papers in Marine Sciences, **36**.

Second International Conference
"Tropical Climatology, Meteorology and Hydrology"
Proceedings edited by
G. Demarée, M. De Dapper, J. Alexandre
pp. 41-60 (2004)

Relationship between the Zonal Circulation over the Equatorial Indian and Pacific Oceans and the East African Lakes : Victoria, Tanganyika and Nyassa-Malawi Level Fluctuations

by

Laurent BERGONZINI* & Yves RICHARD**

KEYWORDS. — East African Lakes ; Lake Level Fluctuations ; Hydrological Variability ; Atmosphere-ocean Interaction ; Teleconnection ; Indian Ocean ; El Niño Southern Oscillation ; Zonal Circulation.

SUMMARY. — The analyses of the Great East African Lakes, Victoria, Tanganyika, and Nyassa-Malawi level records show synchronisms, which can only be accounted for large-scale mechanisms. The relations between lake-level variations and atmospheric circulation indexes are studied. This way, for the period 1946-2000, four indexes are selected to characterize the boreal autumn zonal circulation over the Pacific and Indian Oceans. Over the Indian Ocean two surface Zonal Wind Index (ZWI calculated for October to December) are used. For the Pacific the Southern Oscillation Index (SOI) and the Niño 3 index (during the same quarter) are held to account for the El Niño Southern Oscillation (ENSO). This exploration shows that overall negative correlations between level fluctuations (especially for Victoria and Tanganyika) are only obtained with Indian Ocean circulation indexes. If ZWI are highly correlated with ENSO indexes, except a positive correlation with Nyassa-Malawi, no correlations with ENSO events are shown. It seems tempting to consider that, for the 1946-2000 period, the autumn zonal circulation cell over the Indian Ocean may play a role in the equatorial lake level anomalies. Intense ZWI (abnormally strong western wind) is associated with deficient autumn rainfall followed by lower lake rise. On the

* FRE-CNRS 2566 "ORSAYTERRE", Bât. 504, Université Paris-Sud, 91405 Orsay cedex (France).
** UMR-CNRS 5080, Centre de Recherches de Climatologie, Université de Bourgogne, 21004 Dijon cedex (France).

Second International Conference on

TROPICAL CLIMATOLOGY, METEOROLOGY AND HYDROLOGY

Climate-related Risk Analysis and Sustainable Development in Tropical Areas

Brussels, 13-14 December, 2001

Royal Meteorological Institute
of Belgium

Royal Academy
of Overseas Sciences

Guest Editors : G. Demarée, M. De Dapper, J. Alexandre

2004

ROYAL METEOROLOGICAL INSTITUTE
OF BELGIUM
av. Circulaire / Ringlaan 3
B-1180 BRUSSELS (Belgium)
Tel. : 02.373.05.08
Fax : 02.373.05.28
E-mail : rmi_info@oma.be
Web : www.meteo.be/IRM-KMI/

ROYAL ACADEMY
OF OVERSEAS SCIENCES
rue Defacqzstraat 1/3
B-1000 BRUSSELS (Belgium)
Tel. : 02.538.02.11
Fax : 02.539.23.53
E-mail : kaowarsom@skynet.be
Web : http//www.kaowarsom.be

ISBN 90-75652-36-4
D/2004/0149/5

CONTENTS

Foreword 7

Opening Speech 9

Tropical Meteorology

R. AHMED, Variability and Trends of the Summer Monsoon Rainfall in Bangladesh 15

J. NAITHANI, E. DELEERSNIJDER, P.-D. PLISNIER & S. LEGRAND, Preliminary Results of a Reduced-gravity Model of the Wind-induced Oscillations of the Thermocline in Lake Tanganyika 27

L. BERGONZINI & Y. RICHARD, Relationship between the Zonal Circulation over the Equatorial Indian and Pacific Oceans and the East African Lakes : Victoria, Tanganyika and Nyassa-Malawi Level Fluctuations . 41

Palaeoclimatology & Geomorphic Processes

J. MOEYERSONS, J. NYSSEN, J. DECKERS, H. MITIKU & J. POESEN, The Climatic Significance of Late-Pleistocene and Early- to Middle-Holocene Mass Movements and their Present-day Remobilization in Rwanda and Ethiopia 63

J. HUS, Magnetic Susceptibility : a Proxy of the Palaeoenvironment and Palaeoclimate in Sediments 81

J. NYSSEN, J. POESEN, H. VANDENREYKEN, J. MOEYERSONS, J. DECKERS, H. MITIKU & C. SALLES, Spatial Variability of Rain and its Erosivity in a Tropical Mountain Catchment : Tigray, Northern Ethiopia 95

Agriculture, Food and Weather Prediction

F. Lupo, M. Corlazzoli & E. F. Lambin, Monitoring Natural Disasters and "Hot Spots" of Land-cover Change with SPOT4 Vegetation to Assess Region at Risk 123
E. C. Kipkorir, S. M. Gachuiri, J. Mukabana & D. Raes, Evaluation of the Onset of the Growing Season for Various Climatic Zones in Kenya by means of a Soil Water Balance Method for Different Soil Types . 137
C. B. S. Teh, L. P. Simmonds & T. R. Wheeler, Modelling the Partitioning of Solar Radiation Capture and Evapotranspiration in Intercropping Systems 151

Historical Climatology

M. F. Naranjo, Change in the Hydrological Management of the Mexican Basin during the 16th Century 175
G. P. Konnen, M. Zaiki, F. Baede, T. Mikami, P. D. Jones & T. Tsukahara, Pre-1872 Extension of the Japanese Instrumental Meteorological Observation Series Back to 1819 187
A. Gioda, J. Ronchail, Y. L'Hote & B. Pouyaud, Analyse et variabilité temporelle d'une longue série de pluies des Andes en relation avec l'Oscillation Australe (La Paz, 3 658 m, 1891-2000) 199
A. Drebs, Early Weather Observations in Olukonda, Namibia, 1905-1926.. 219

Tropical Hydrology

V. Thanh Tam, F. De Smedt & O. Batelaan, Estimation of Underground Rivers in a Tropical Karst Area by way of a Multithematic Study ... 231
G. R. Demaree, Intensity-Duration-Frequency (IDF) Curves for Yangambi, Congo, based upon Long-term High-frequency Precipitation Data Set (Part I) 245
B. Mohymont & G. R. Demaree, The Establishment of Intensity-Duration-Frequency Curves for Precipitation in Yangambi, Congo (Part II) 253
Y. Seleshi, Design Flood Estimation under Inadequate Data — a Case Study 267

Tropical Climatology

M. Muchinda, Drought Incidence in Zambia over the Thirty-year Period 1970/1971 - 1999/2000 281
J. C. Moliba Bankanza, Classification des régimes pluviométriques en République Démocratique du Congo et en Angola 295
E. Nieplova, Long-term Temperature and Precipitation Variability and Trends in Kuwait 307
P. Ozer, B. Tychon, A. Ozer & R. Paul, L'enseignement en gestion des risques naturels 321
P. Ozer, Can Dust Variability be a Regional Indicator of Land Degradation Trend in Arid and Semi-arid Areas ? Analysis in the Sahel 331
S. Sene & P. Ozer, Are the 1999 and 2000 Urban Floods in Senegal due to Exceptional Rainfall Events ? 345
E. V. Sokolikhina, N. N. Sokolikhina & E. K. Semenov, The Assessment of the Connection between the Atmospheric Circulation and the Sea Surface Temperature (SST) of the Equatorial Pacific for Synoptic Scale Processes using the Singular Value Decomposition Method (SVD) 353